ORIGINAL ARTICLE

Presence of B Cells in Tertiary Lymphoid Structures Is Associated with a Protective Immunity in Patients with Lung Cancer

Claire Germain[1,2,3], Sacha Gnjatic[4,5], Fella Tamzalit[1,2,3], Samantha Knockaert[1,2,3], Romain Remark[1,2,3], Jérémy Goc[1,2,3], Alice Lepelley[1,2,3], Etienne Becht[1,2,3], Sandrine Katsahian[6,7], Geoffray Bizouard[6], Pierre Validire[1,8], Diane Damotte[1,2,3,9], Marco Alifano[10], Pierre Magdeleinat[10,11], Isabelle Cremer[1,2,3], Jean-Luc Teillaud[1,2,3], Wolf-Herman Fridman[1,2,3,12], Catherine Sautès-Fridman[1,2,3], and Marie-Caroline Dieu-Nosjean[1,2,3]

[1]Laboratory "Immune Microenvironment and Tumors" and [7]Laboratory "Information Sciences to Support Personalized Medicine," INSERM U872, Cordeliers Research Center, Paris, France; [2]University Pierre and Marie Curie, UMRS 872, Paris, France; [3]University Paris Descartes, UMRS 872, Paris, France; [4]Division of Hematology, Oncology and Immunology, The Tisch Cancer Institute at Hess CSM, New York, New York; [5]Ludwig Institute for Cancer Research Ltd., New York Branch at Memorial Sloan-Kettering Cancer Center, New York, New York; [6]Clinical Research Unit, Henri Mondor Hospital, Paris, France; [8]Department of Pathology and [11]Department of Thoracic Surgery, Institut Mutualiste Montsouris, Paris, France; [9]Department of Pathology and [10]Department of General Surgery, Hotel Dieu Hospital, AP-HP, Paris, France; and [12]Department of Immunology, Hospital European Georges Pompidou, AP-HP, Paris, France

Abstract

Rationale: It is now well established that immune responses can take place outside of primary and secondary lymphoid organs. We previously described the presence of tertiary lymphoid structures (TLS) in patients with non–small cell lung cancer (NSCLC) characterized by clusters of mature dendritic cells (DCs) and T cells surrounded by B-cell follicles. We demonstrated that the density of these mature DCs was associated with favorable clinical outcome.

Objectives: To study the role of follicular B cells in TLS and the potential link with a local humoral immune response in patients with NSCLC.

Methods: The cellular composition of TLS was investigated by immunohistochemistry. Characterization of B-cell subsets was performed by flow cytometry. A retrospective study was conducted in two independent cohorts of patients. Antibody specificity was analyzed by ELISA.

Measurements and Main Results: Consistent with TLS organization, all stages of B-cell differentiation were detectable in most tumors. Germinal center somatic hypermutation and class switch recombination machineries were activated, associated with the generation of plasma cells. Approximately half of the patients showed antibody reactivity against up to 7 out of the 33 tumor antigens tested. A high density of follicular B cells correlated with long-term survival, both in patients with early-stage NSCLC and with advanced-stage NSCLC treated with chemotherapy. The combination of follicular B cell and mature DC densities allowed the identification of patients with the best clinical outcome.

Conclusions: B-cell density represents a new prognostic biomarker for NSCLC patient survival, and makes the link between TLS and a protective B cell–mediated immunity.

Keywords: non–small cell lung cancer; tumor immunology; follicular B cell; prognostic marker; antibody

(Received in original form September 8, 2013; accepted in final form January 26, 2014)

Supported by the Institut National de la Santé et de la Recherche Médicale, the Fondation ARC pour la Recherche sur le Cancer (SL220110603483), the Cancéropôle Ile-de-France, the University Paris-Descartes, the University Pierre and Marie Curie, the Institut National du Cancer (2011-1-PLBIO-06-INSERM 6-1, PLBIO09-088-IDF-KROEMER), Cancer Research for Personalized Medicine, and Labex Immuno-Oncology (LAXE62_9 UMS872 FRIDMAN). S.G. was supported by a grant from the Cancer Research Institute as part of the Cancer Vaccine Collaborative.

Author Contributions: M.-C.D.-N. designed the research. C.G., S.G., F.T., R.R., A.L., S.K., and G.B. performed the research. P.V., D.D., M.A., and P.M. provided fresh human specimens and patient enrollment. C.G., S.G., F.T., R.R., J.G., A.L., D.D., S.K., and M.-C.D.-N. analyzed the data. D.D., I.C., J.-L.T., W.-H.F., and C.S.-F. critically revised the manuscript for important intellectual content. W.-H.F., C.S.-F., and M.-C.D.-N. obtained funding. C.G. and M.-C.D.-N. wrote the manuscript. All authors read and approved the final version of the manuscript.

Correspondence and requests for reprints should be addressed to Marie-Caroline Dieu-Nosjean, Ph.D., Immune Microenvironment and Tumors, INSERM UMRS 872, Cordeliers Research Center, 15, Rue de l'école de Médecine, F-75270 Paris cedex 06, France. E-mail: mc.dieu-nosjean@crc.jussieu.fr

This article has an online supplement, which is accessible from this issue's table of contents at www.atsjournals.org

Am J Respir Crit Care Med Vol 189, Iss 7, pp 832–844, Apr 1, 2014

Originally Published in Press as DOI: 10.1164/rccm.201309-1611OC on January 31, 2014
Internet address: www.atsjournals.org

At a Glance Commentary

Scientific Knowledge on the Subject: The role of tumor-infiltrating B cells is controversial.

What This Study Adds to the Field: Here, we demonstrate that B cells organized into tertiary lymphoid structures exhibit features of an ongoing humoral immune response, and that their high density is associated with the long-term survival of patients with non–small cell lung cancer. The presence of both types of antigen-presenting cells, mature dendritic cells and B cells, in tertiary lymphoid structures strongly predicts the outcome of patients. The low density of both follicular B cells and mature dendritic cells allows the identification of patients at high risk of poor survival.

Tumors support a complex microenvironment characterized by many immune cell populations, reflecting the capacity of the immune system to sense tumor cells. Numerous studies have described the existence of naturally occurring tumor antigen (TA)-specific T-cell and B-cell responses, including TA-specific antibodies (Abs) (1–6). The role of T cells especially in the control and eradication of tumors has been largely documented (7, 8). Notably, several clinical studies have demonstrated that a high density of tumor-infiltrating T cells is associated with an increased median survival of cancer patients (9, 10). In contrast, the role played by the humoral immune response and B cells is still a matter of debate (11–15). Although in mice many studies assigned B cells with a protumoral function, mainly based on the maintenance of a deleterious chronic inflammation (16–19), several studies in humans associated a high density of tumor-infiltrating B cells and plasma cells (PCs) with a favorable clinical outcome, and reported a positive correlation between the expression of B-cell related genes and disease-free survival (20–22).

Previously, we described tertiary lymphoid structures (TLS) in non–small cell lung cancer (NSCLC) tumors, encompassing follicular B cells and clusters of DC-Lamp$^+$ mature dendritic cells (DCs) and T cells (23). We showed that the density of DC-Lamp$^+$ mature DCs correlated with long-term survival of patients with early-stage NSCLC. TLS, initially described in autoimmune disorders, infectious diseases, and graft rejection (24), are transient lymphoid structures induced on chronic inflammation in nonlymphoid tissues. In autoimmune diseases, the presence of TLS was associated with disease exacerbation and poor prognosis (25), whereas during infection, T- and B-cell responses initiated in TLS were protective (26). To date, studies understanding the role of TLS in the induction of a humoral immune response in human cancer are lacking.

In the present work, we fully characterize tumor-infiltrating B-cell subsets in NSCLC. We demonstrate that B-cell follicles in TLS present features of an ongoing humoral immune response, that a high follicular B-cell density is associated with longer survival in patients with NSCLC, and that the combination of follicular B-cell and mature DC densities further enhanced the prognostic value. Some of the results of this study have been previously reported as a poster during the 15th International Congress of Immunology in Milan, Italy (August 22–27, 2013) (27).

Methods

Patients

A retrospective study was performed on formalin-fixed, paraffin-embedded NSCLC tumor samples, comprised of 74 untreated patients with early-stage NSCLC (*see* Table E1 in the online supplement) and 122 patients with advanced-stage NSCLC, treated with neoadjuvant chemotherapy (*see* Table E2). Fresh tumor biopsies were retrieved from 61 patients with NSCLC for a prospective study. Nontumoral lymph nodes (LNs) were obtained from patients undergoing surgery for cardiac diseases. Peripheral blood was obtained from healthy volunteers. Additional details are provided in the online supplement.

Immunohistochemistry

Serial sections of paraffin-embedded NSCLC tumors were stained as previously described (28), using antigen retrieval conditions, Abs, and reagents listed in Table E3. Single stainings were counterstained with hematoxylin.

Methods for Cell Quantification

Cell quantification was performed across whole tumor section. Mature DC quantification was determined as previously described (23) and expressed as the number of DC-Lamp$^+$ DCs per tumor intermediate-power field (IPF) (original magnification ×100), with SEMs. Follicular CD20$^+$ B-cell quantification was determined using a Nikon Eclipse 80i microscope operated with Nikon NIS Elements BR software (Amsterdam, Netherlands) and expressed as the surface of CD20$^+$ B-cell follicles in square millimeter per tumor IPF, with SEMs.

Ex Vivo Culture of B Cells

Mononuclear cells were isolated from fresh lung tumor specimens as previously described (28). After cell sorting, total CD19$^+$ B cells were cultured in the presence of Pansorbin (*Staphylococcus aureus* cell extract; Merck, Darmstadt, Germany) and the supernatant (SN) was recovered every 3 days until Day 20 (*see* online supplement for details).

Flow Cytometry

Multiple stainings on isolated mononuclear cells were performed using Abs against B-cell markers (*see* Table E3), as previously described (28).

TA Specificity

B-cell SN reactivity against a series of 33 TAs (*see* Table E4) was evaluated by ELISA, as previously described (29). When possible, patient serum was also tested. Levels of TA-bound IgG, IgA, IgD, IgE, and IgM were determined and expressed as reciprocal titers (*see* online supplement).

Statistical Analysis

Patients were stratified into two groups according to a high or low density of follicular B cells and mature DCs, using the "minimum *P* value" approach, which determines the cutoff value for the best separation of patients referring to their outcome (outcome-oriented approach), as previously described (*see* Figure E1) (30). Groups of patients were appointed using the following cutoffs: 0.0255 mm^2 of follicular CD20$^+$ B cells/tumor IPF (fifth decile; *see* Figure E1A) and 1.65 DC-Lamp$^+$ DCs/tumor IPF (third decile; *see* Figure E1B) for patients with early-stage NSCLC, 0.042 mm^2 of follicular CD20$^+$ B cells/tumor IPF (sixth decile; *see* Figure E1C)

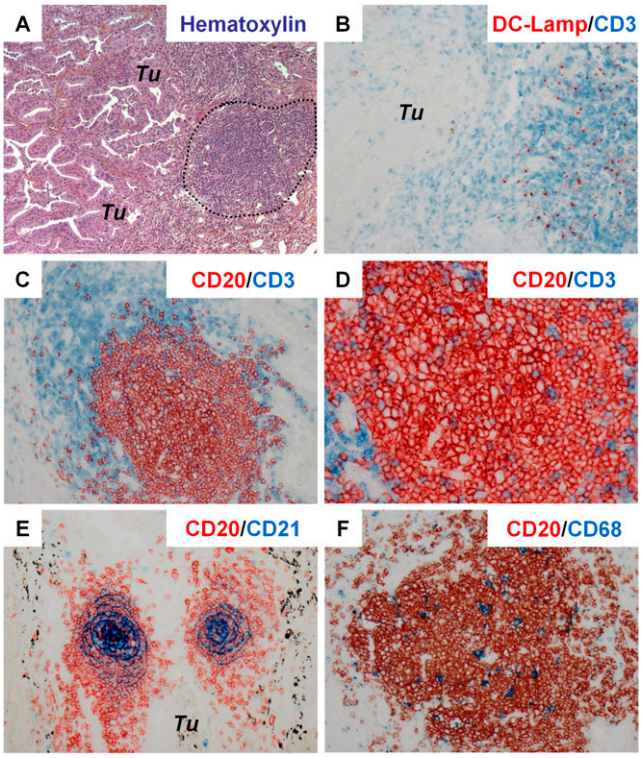

Figure 1. Characterization of immune cells within tertiary lymphoid structures (TLS). Counter-staining (*A*) and double immunostainings (*B–F*) on paraffin-embedded lung tumor sections. (*A*) Presence of TLS (*dashed line*) in the tumor microenvironment. TLS are composed of the following: (*B*) a T-cell rich area where DC-Lamp$^+$ mature dendritic cell (DCs) (*red*) home exclusively and form clusters with CD3$^+$ T cells (*blue*), and (*C*) a CD20$^+$ B-cell rich area (*red*) adjacent to a CD3$^+$ T-cell zone (*blue*). B-cell follicles are infiltrated by a subset of CD3$^+$ T cells (*blue*, *D*), CD21$^+$ follicular DCs organized in a network (*blue*, *E*), and CD68$^+$ tingible-body macrophages (*blue*, *F*). Original magnification: *A*, ×100; *B*, *C*, *E*, and *F*, ×200; *D*, ×400. Tu = tumor nest.

and 10 DC-Lamp$^+$ DCs/tumor IPF (sixth decile; *see* Figure E1D) for patients with advanced-stage NSCLC. Disease-specific survival (DSS) curves were estimated by Kaplan-Meier method and differences between patient groups were calculated using the log-rank test, corrected using the formula proposed by Altman and coworkers (31). Cox model was used for univariate analysis and differences between categories were calculated using the Wald test. A *P* value less than 0.05 was considered statistically significant. Additional details are provided in the online supplement.

Results

TLS Are Composed of the Same Contingent of Immune Cells as Secondary Lymphoid Organs

We previously reported the presence of TLS in human lung tumors, which we called tumor-induced bronchus-associated lymphoid tissues (23). Because similar structures were afterward described in tissues other than lung and in several inflammatory pathologies, we now use the terminology used in the literature, namely TLS (32). These TLS were mainly observed within tumor stroma, at the invasive margin of the tumor, and between tumor nests (*see* Figure E2). To study the role of the B-cell compartment within TLS, we first characterized immune cells surrounding B-cell follicles by immunohistochemistry (Figure 1A). As described in canonical lymphoid organs, we observed T-cell rich areas composed of clusters of CD3$^+$ T cells and DC-Lamp$^+$ mature DCs (Figure 1B), whereas most B cells, visualized with the mature B-cell marker CD20, segregated into follicles (Figure 1C). Many non-CD20$^+$ cells were also detectable within the B-cell follicles: few CD3$^+$ T cells (Figure 1D), a network of CD21$^+$ follicular DCs (Figure 1E), and a population of specialized CD68$^+$ macrophages (tingible-body macrophages; Figure 1F). These observations indicate that the presence and segregation of immune cells in TLS are the same as observed in secondary lymphoid organs, suggesting adaptive immune responses may take place within NSCLC-associated TLS.

B-Cell Areas of TLS Have Features of an Ongoing Humoral Immune Response

The segregation of T- and B-cell areas in secondary lymphoid organs is mandatory for the development of both high-affinity class-switched Abs and memory humoral immune responses. To determine if TLS could be sites for immune responses, we first assessed by immunohistochemistry B-cell differentiation stages in lung tumors, and compared it with secondary lymphoid organs. As in LN follicles (Figure 2A), we showed in NSCLC-associated TLS an accumulation of IgD$^+$ naive B cells in a restricted area corresponding to the mantle (Figure 2B). The mantle surrounded a germinal center (GC), defined by the presence of CD23$^+$ cells (Figures 2C and 2D in LN and TLS, respectively). GC–B cells expressed AID (Figures 2E and 2F in LN and TLS, respectively), the critical enzyme for somatic hypermutation (SHM), class switch recombination (CSR), and gene conversion of immunoglobulin genes. GC–B cells were positive for the proliferation marker Ki67 (Figures 2G and 2H) and Bcl6 (Figures 2I and 2J), but did not express the antiapoptotic protein Bcl2 (Figures 2K and 2L) both in LN and TLS. PCs stained with anti-CD138 Ab could be detected at the periphery of B follicles in LN (Figure 2M) and TLS (Figure 2N), and in the stroma and fibrosis of the tumor (data not shown).

We further characterized and compared by flow cytometry intratumoral B-cell subsets with other anatomic sites, such as peripheral blood, LN, and nontumoral distant lung from patients with NSCLC and healthy donors (except for lung tissue). To visualize B cells we used here the pan–B cell marker CD19, expressed on all B-cell stages, whereas CD20 is known to be extinguished on PCs (33). Fc-receptor–expressing cells, mainly CD14-positive monocytes and macrophages, were systematically excluded from the analysis to avoid false positives, using an anti-CD14

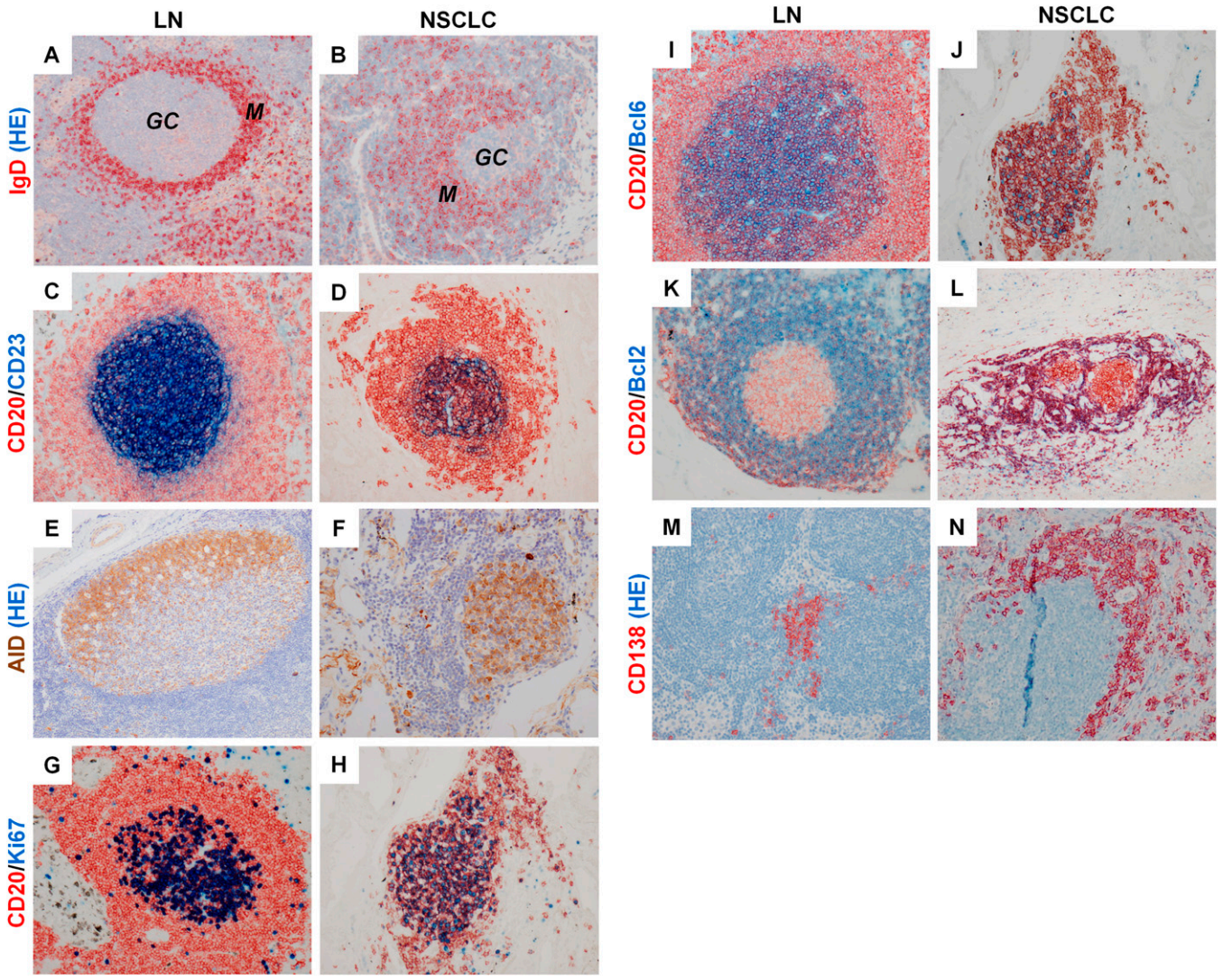

Figure 2. Characterization of B-cell subsets within and outside tertiary lymphoid structures (TLS). Single (*A*, *B*, *E*, *F*, *M*, and *N*) and double (*C*, *D*, and *G–L*) immunostainings on paraffin-embedded lymph node (LN) (*left column*) and non–small cell lung cancer (NSCLC) tumor (*right column*) sections. TLS B-cell areas present features of secondary follicles of reactive LNs (*A*), because they are composed of a mantle of IgD^+ naive B cells (*red*, *B*) surrounding a germinal center. As in LNs (*C*, *E*, *G*, *I*, and *K*), germinal center B cells express CD23 (*blue*, *D*), AID (*brown*, *F*), Ki67 (*blue*, *H*), and Bcl6 (*blue*, *J*) but not Bcl2 (*blue*, *L*). In NSCLC tumor, $CD138^+$ plasma cells (*red*, *N*) are detected at the periphery of TLS and in the stroma of the tumor. Original magnification: *A–N*, ×200. GC = germinal center; M = mantle.

Ab. B-cell subsets were identified based on the differential expression of IgD and CD38 (34), including $IgD^-CD38^{++}CD138^-$ and $IgD^-CD38^{++}CD138^+$ (more mature) PCs (35). Every stage of B-cell differentiation was observed in tumors; however, their distribution was largely different from that in blood and LN from patients with NSCLC (Figures 3A and 3B). Memory B cells represented the predominant B-cell subset, irrespective of anatomic location. The second major population was naive B cells in blood and LN, whereas it was PCs in tumors (Figure 3B; 27.7, 17.2, and 7.5% of naive B cells and 1.5, 2.3, and 16.5% of PCs in blood, LNs, and tumors; absolute numbers for tumors are provided in Table E5). An intermediate distribution was observed in distant nontumoral lung, with equivalent percentages of naive B cells and PCs (Figure 3B; 8.8 and 10.6%, respectively). As opposed to what was observed in healthy donors, the ratio of naive/memory B cells was in favor of memory B cells in patients with NSCLC, both in blood and LNs (*see* Figure E3). No statistical difference was observed regarding GC–B cells between the different anatomic locations. The differential expression of additional markers (the activation marker CD23, the memory marker CD27, and the GC/centroblast marker CD77) allowed us to study the distribution of naive (Bm1 and Bm2), GC (Bm3 and Bm4), and memory (early Bm5 and late Bm5) B-cell subsets (34) in tumors compared with LNs from patients with NSCLC. Only a trend in favor of Bm1 versus Bm2 was seen in lung tumors versus LN (Figure 3C). Finally, we observed a significant correlation between the percentages of PCs and GC-B cells in

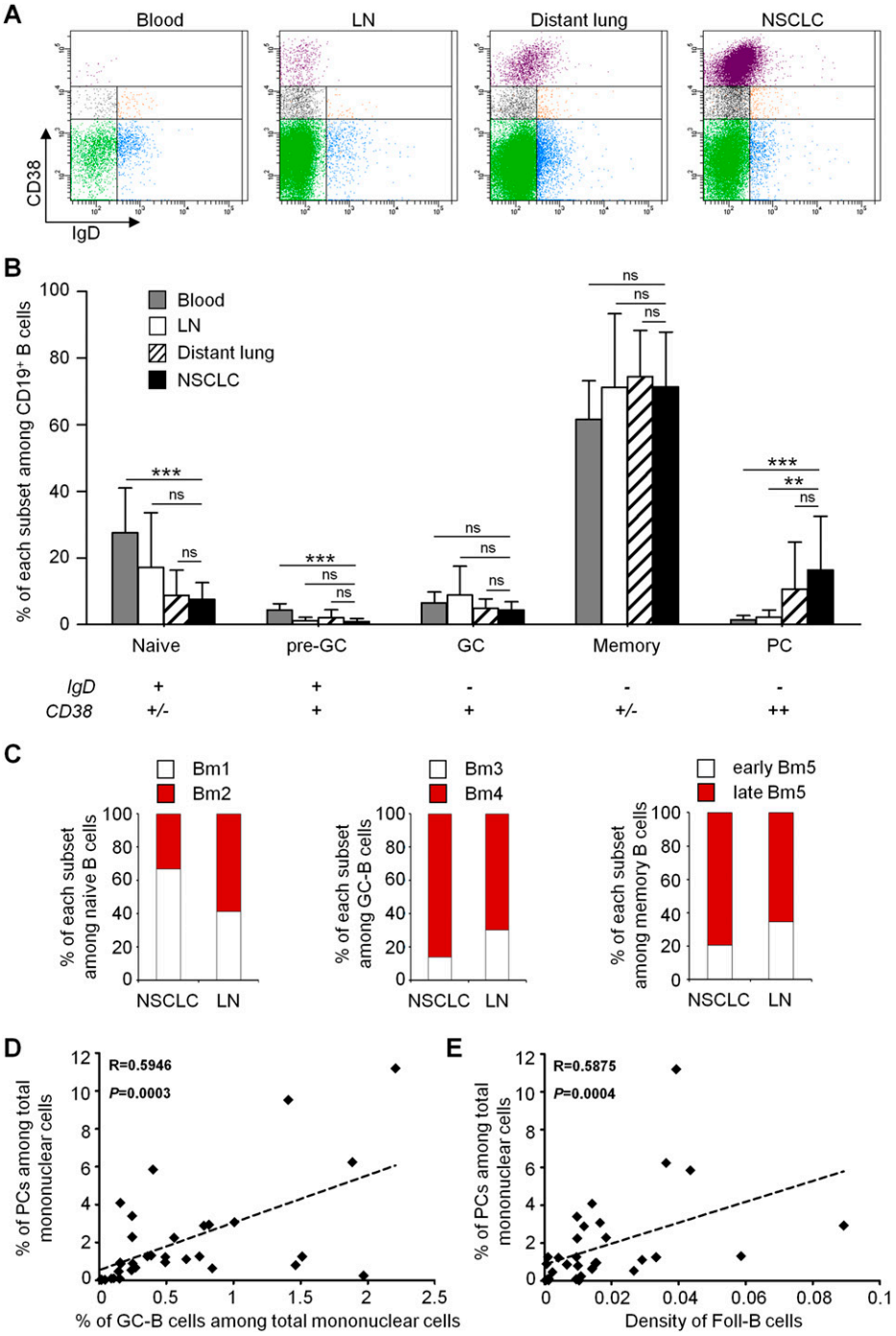

Figure 3. Characterization of the B-cell subsets infiltrating lung tumors and comparison with nontumoral sites. Flow cytometry analysis of B-cell subsets in lung tumors (n = 33) compared with distant nontumoral lungs (n = 13), draining lymph nodes (n = 6), and peripheral blood (n = 8) from patients with non–small cell lung cancer. (*A*) Representative dot plots and (*B*) mean ± SD of the percentages of each B-cell subset among total $CD14^-$ $CD19^+$ B cells, based on the differential expression of IgD and CD38, in the different anatomic sites. $IgD^+CD38^{+/-}$, naive B cells; IgD^+CD38^+, pre-GC B cells; IgD^-CD38^+, GC B cells; $IgD^-CD38^{+/-}$, memory B cells; IgD^-CD38^{++}, PCs. Statistical significance between sites was determined by Mann-Whitney test. ns = not significant; $^{**}P < 0.005$; $^{***}P < 0.0005$. (*C*) Different differentiation stages of naive B cells (IgD^+ $CD38^-$ $CD27^-$ $CD23^-$ Bm1 and IgD^+ $CD38^-$ $CD27^-$ $CD23^+$ Bm2, *left*), GC B cells (IgD^- $CD38^+$ $CD23^-$ $CD27^-$ $CD77^+$ Bm3 and IgD^- $CD38^+$ $CD23^-$ $CD27^-$ $CD77^-$ Bm4, *center*), and memory B cells (IgD^- $CD23^-$ $CD27^+$ $CD38^+$ early Bm5 and IgD^- $CD23^-$ $CD27^+$ $CD38^-$ late Bm5, *right*) in lung tumors (n = 18) and matched lymph nodes (n = 6) from patients with non–small cell lung cancer. (*D*) Correlation between the percentage of PCs and the percentage of GC B cells among total mononuclear cells in lung tumors (n = 33). (*E*) Correlation between the percentage of PCs among total mononuclear cells and the density of follicular B cells in the tumor section (n = 32). Statistical significance was determined by Spearman test. Foll-B (cell) = follicular B (cell); GC = germinal center; LN = lymph node; NSCLC = non–small cell lung cancer; PC = plasma cell; pre-GC = pre-germinal center.

fresh lung tumors ($R = 0.5946$; $P = 0.0003$) (Figure 3D) but also with the density of follicular B cells in the corresponding paraffin-embedded lung tumor sections ($R = 0.5875$; $P = 0.0004$) (Figure 3E), suggesting that most PCs were differentiated within NSCLC-associated TLS.

The presence of all B-cell differentiation stages in NSCLC tumors is in accordance with their *in situ* organization in TLS. Early-activated B cells undergo active proliferation in B-cell follicles where SHM and CSR machineries are activated, suggesting that TLS may be an active site for the generation of a humoral immunity.

Production of Tumor-Specific Abs by Intratumoral PCs

To determine whether tumor-infiltrating PCs may have a functional role in tumor recognition, we evaluated the capacity of their Abs to recognize common TAs known to elicit spontaneous immune responses in cancer patients (36). SNs of B-cell cultures from 34 patients with NSCLC were analyzed by ELISA for IgG and IgA binding to a series of 33 TAs, including mostly cancer/testis antigens (NY-ESO-1, LAGE-1, MAGEs, SSXs, and so forth), mutational and stem-cell antigens (TP53, SOX2), endogenous retroviral antigens (GAG-HERV-K), along with a negative control antigen (DHFR) (*see* Table E4). Reactivity was detected against 21 out of the 33 TAs tested (Figure 4A and Table 1). Some IgG reactive SNs also displayed IgA reactivity against the same TA (Table 1). Over 41% of SNs (14 out of 34) displayed reactivity against at least one TA (Table 1). Some SNs showed multiple antigen-specific IgG and IgA reactivity, such as P5, P11, and P22 with up to six to seven different TAs recognized. The most frequently recognized TAs were LAGE-1 (5 out of 14 SNs); then MAGEA1, MAGEC2, TP53 (3 out of 14 SNs); NY-ESO-1; and other MAGE antigens (MAGEA3 and MAGEA4, 2 out of 14 SNs). A low IgA reactivity against CT47 was observed in PBMC1 control SN. Reactivity against this TA has already been described in healthy donor sera (37).

We further analyzed the strong reactivity observed for P22 SN against NY-ESO-1, by assessing its capacity to recognize a series of 17 overlapping peptides along the NY-ESO-1 molecule. The anti–NY-ESO-1 response was polyclonal, because at least three different areas of NY-ESO-1 molecule were recognized (Figures 4B and 4C). Similar results were obtained with P21 SN, displaying reactivity against at least four different areas of TP53 molecule (*see* Figure E4). Ab titers were observed as early as the third day of culture, and remained constant over time (Day 3–20; Figure 4C). The reactivity observed in P22 SN against NY-ESO-1 (Figures 4A and 4C) was mainly ascribed to a mixture of IgG and IgA but also IgM (Figure 4D). Next, we asked whether the antigen-specific Ab responses detected in primary tumors reflected overall seroreactivity from circulating blood. Two out of six patients had evidence of Abs against the same antigens in NSCLC SN and serum (Figure 4E).

In parallel, we analyzed the expression of the TAs in matched tumor samples by reverse transcriptase polymerase chain reaction (*see* online supplement). We observed a correlation between TA mRNA expression and IgG reactivity in two-thirds of the cases (data not shown).

Finally, we evaluated follicular B-cell densities in the paraffin-embedded tumors corresponding to the evaluated B-cell SN (stratification of patients according to the density of $CD20^+$ follicular B cells is detailed next). We observed that 44% (12 out of 27) of the SNs coming from tumors with high densities of follicular B cells displayed Ig reactivity against at least 1 out of 33 TAs tested, whereas only 29% (2 of 7) of the SNs coming from tumors with low follicular B-cell densities displayed an Ig reactivity (data not shown).

All together, these data demonstrate that TAs expressed by tumor cells are recognized by IgG and IgA-secreting PCs in the tumors.

Density of Follicular B Cells Correlates with Long-Term Survival, and a Synergistic Effect Is Observed When Combined with Mature DC Density

Because the density of mature DCs was shown to be associated with a favorable prognosis in patients with NSCLC (23), we investigated correlations between follicular B-cell and mature DC densities, and whether they were associated with good clinical outcome (Figure 5). Two independent patient cohorts were evaluated: 74 untreated patients with early-stage NSCLC (*left column*) and 122 patients with advanced-stage NSCLC treated with neoadjuvant chemotherapy (*right column*).

The global increase of follicular B-cell density was associated with an overall increase in mature DC density. Based on cutoffs determined by the minimum *P* value approach (*see* Figure E1), we discriminated between patients with a high or a low density of follicular B cells and/or mature DCs. In the cohort of patients with early-stage NSCLC, 47% of patients (35 out of 74) were characterized as having a high density of both populations ("Foll-B/DC Hi Hi"), and 23% of patients (17 out of 74) a low density of both populations ("Foll-B/DC Lo Lo") (Figures 5A and 5G). Similar results were obtained in the advanced-stage NSCLC cohort, with 22% of "Foll-B/DC Hi Hi" patients (27 out of 122) and 39% "Foll-B/DC Lo Lo" patients (47 out of 122) (Figures 5B and 5H). However, the existence of "Foll B/DC mix" patients was observed in both cohorts: 17 "Foll-B/DC Lo Hi" patients and 5 "Foll-B/DC Hi Lo" patients (22 patients; 30%) in the early-stage NSCLC cohort (Figures 5A and 5G); 25 "Foll-B/DC Lo Hi" patients and 23 "Foll-B/DC Hi Lo" patients (48 patients; 39%) in the advanced-stage NSCLC cohort (Figures 5B and 5H). In both cohorts, patient distribution within the different Foll-B and DC groups was not influenced by tumor histologic subtypes (Figures 5A and 5B; *see* Tables E6–E9), suggesting that these parameters are independent.

The Kaplan-Meier curves indicated that "Foll-B Hi" patients have a prolonged survival as compared with "Foll-B Lo" patients ($P = 0.04$ for patients with early-stage NSCLC) (Figure 5C). The 4-year DSS rates were 97% among "Foll-B Hi" patients versus 62% among "Foll-B Lo" patients. A strong benefit in terms of survival was also observed for patients with advanced-stage NSCLC, even if significance was not reached (median DSS = 56 mo for "Foll-B Hi" *vs.* 23 mo for "Foll-B Lo" patients; $P = 0.06$) (Figure 5D). The density of mature DCs was also associated with a favorable outcome in both cohorts ($P = 0.003$ in patients with early-stage NSCLC [Figure 5E], and $P = 0.01$ in treated patients with late-stage NSCLC [Figure 5F]).

We next combined the two immune populations. "Foll-B/DC Hi Hi" patients had the highest rate and median survival. One hundred percent of patients with early-stage NSCLC ($P < 0.04$) (Figure 5G), and 55% of treated patients with advanced-stage NSCLC ($P = 0.007$) (Figure 5H) were

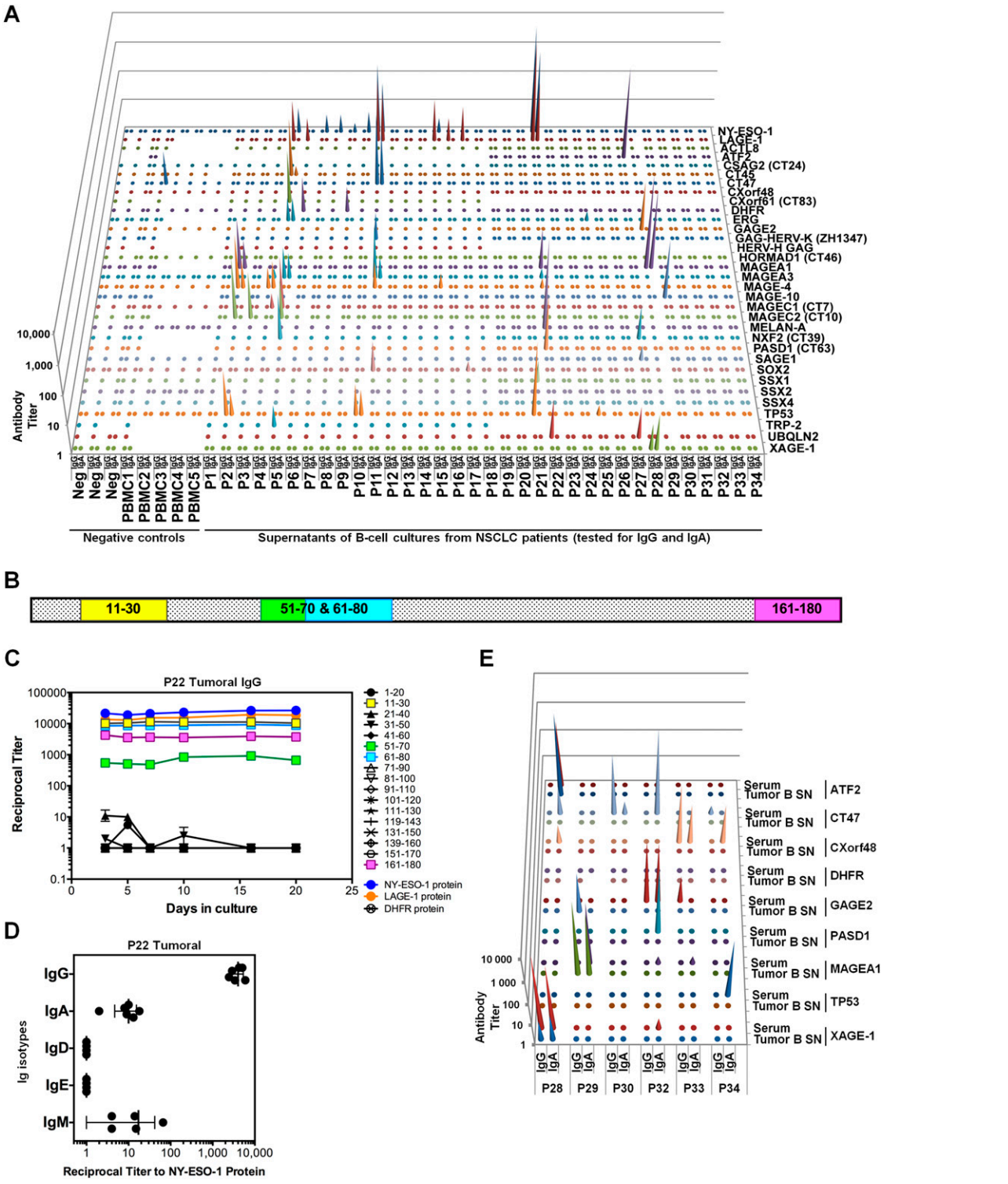

Figure 4. Reactivity of antibodies secreted by tumor-infiltrating B cells against tumor antigens. Freshly sorted tumor-infiltrating B cells from 34 tumors were cultivated *ex vivo*. (*A*) Supernatants (SNs) containing secreted IgG and IgA antibodies (*x* axis) were tested for reactivity against 33 tumor antigens (TAs) (recombinant full-length proteins, *z* axis) by ELISA. Peaks indicate average titers (*y* axis) of at least two repeats (i.e., maximal dilution of SNs still significantly reacting compared with a negative control SN [Neg, complete culture medium without B cells; peripheral blood mononuclear cell (PBMC), SN of cultured B cells from PBMCs of a healthy individual]). Statistical significance between the total number of reactivities detected in the control group (PBMCs) and the total number of reactivities detected in the patient group was determined by Fisher test ($P = 0.0395$). (*B*) Schematic mapping of 20-mer overlapping NY-ESO-1 peptides recognized in ELISA by P22 SN along the sequence of NY-ESO-1. (*C*) IgG antibody titers of P22 SN against individual

Table 1: IgG and IgA Antibody Reactivity against Tumor Antigens

	SN														
TA	**P5**	**P22**	**P11**	**P2**	**P28**	**P29**	**P21**	**P3**	**P6**	**P10**	**P15**	**P17**	**P27**	**P30**	**Total out of 14**
LAGE-1	+	+++	++								+	+			5
MAGEA1		+		+		+++									3
MAGEC2	+			++				+							3
TP53				+			++			+					3
NY-ESO-1		+++	+												2
MAGEA3	+		+												2
MAGEA4			+	+											2
UBQLN2		+											+		2
NXF2	+				+										2
MELAN-A		+++													1
ATF2					+++										1
CT47			++												1
MAGEA10														+	1
PASD1		+													1
GAGE2						+									1
CT45	+														1
MAGEC1	+														1
CXorf61	+														1
XAGE-1					+										1
SOX2			+												1
DHFR									+						1
Total	7	6	6	4	3	2	1	1	1	1	1	1	1	1	

Definition of abbreviations: SN = supernatant; TA = tumor antigen.
List of the 21 TAs recognized by IgG and/or IgA antibodies in 14 out of the 34 B-cell SNs tested. Only SNs displaying significant reactivity (titer >10) against at least 1 of the 33 tested TAs are represented. Last line indicates the number of TAs recognized by the considered SN. SNs are ranked from the highest number (on the left) to the lowest number (on the right) of TAs recognized. Last column indicates the number of SNs displaying reactivity against the considered TA. TAs are ranked from the highest number (on the top) to the lowest number (on the bottom) of reactive SNs. Bold = double IgG-IgA reactivity with IgG greater than IgA; + = reciprocal titer comprised between 10 and 99; ++ = reciprocal titer comprised between 100 and 999; +++ = reciprocal titer greater than 999.

alive after a follow-up of 50 and 60 months, respectively. In contrast, "Foll-B/DC Lo Lo" patients had the worst rate and median survival. Only 38% of patients with early-stage NSCLC were alive after a follow-up of 50 months, with a median DSS of 42 months, and only 10% of patients with advanced-stage NSCLC were alive after a follow-up of 60 months, with a median DSS of 22 months. "Foll-B/DC mix" patients were at intermediate risk of death, with 82% and 42% of patients alive in early-stage and advanced-stage NSCLC cohorts, respectively.

These data were confirmed through cumulative impact analyses demonstrating no significant difference between patients who died from other causes than NSCLC in each group among each cohort (*see* Figure E5). By univariate analyses, we showed that the density of each immune cell type was highly associated with patient survival, and the combination of both biomarkers was the best predictor for survival, compared with standard clinical parameters (Tables 2 and 3, for early-stage and advanced-stage NSCLC cohorts, respectively).

In conclusion, the density of these two antigen-presenting cell types is highly predictive of DSS in early-stage NSCLC and late-stage NSCLC, independently of the preoperative treatment received. More importantly, low densities of both follicular B cells and mature DCs allowed the identification of a group of patients with the worst clinical outcome.

Discussion

Numerous studies demonstrated in several cancer types that elevated immune cell infiltration correlates with a favorable clinical outcome (8–10, 38). Previously, we extended this concept by describing for the first time the presence of TLS in the tumor stroma of patients with NSCLC (23). We showed that these TLS were composed of mature DCs forming clusters with T cells, surrounded by B-cell follicles, and that a high TLS density of DCs correlated with longer survival in early-stage NSCLC. In the present study, we analyzed B-cell organization, differentiation, and prognostic impact in NSCLC. We first observed that follicular B cells included GC–B cells, characterized by a network of follicular DCs and $Ki67^+$ proliferating B cells. The expression of AID and Bcl6 suggests that SHM and CSR machineries are activated, processes that are required for the generation of effector and memory B cells after B-cell activation (39). The presence of all B-cell stages, including $CD38^+$ IgD^- GC–B cells, with a majority of memory B cells and variable percentages of PCs, was

Figure 4. (Continued). 20-mer overlapping NY-ESO-1 peptides (as indicated), sampled from Day 3–20 of *ex vivo* culture. Full-length NY-ESO-1, LAGE-1, and DHFR proteins were used as controls. (*D*) Immunoglobulin classes from P22 SN reacting with NY-ESO-1 protein. Each *dot* represents a day of B-cell culture, from Day 3–20. Titers against IgG, IgA, and IgM were considered significant. (*E*) For six patients listed in *A*, IgG and IgA reactivity against TAs listed in *A* were compared between SNs of B-cell cultures and serum from the same patient. Only antigens that showed reactivity in at least one SN are shown (*z* axis), along with negative control antigen DHFR. Neg = negative control.

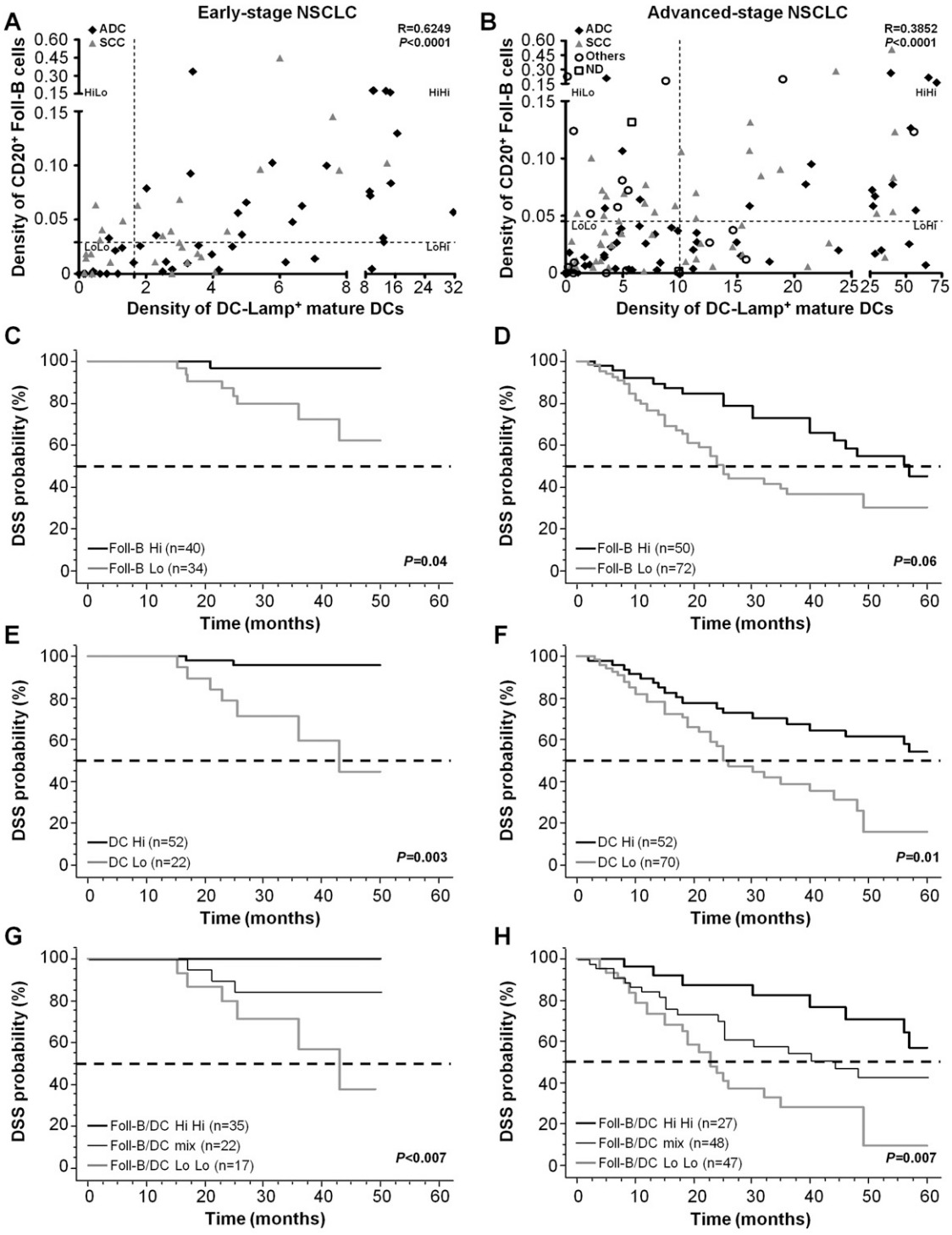

Figure 5. Prognostic value of tertiary lymphoid structure dendritic cells (DCs) and B cells in patients with non–small cell lung cancer (NSCLC). Correlation between the densities of follicular $CD20^+$ B cells versus DC-$Lamp^+$ mature DCs among the two retrospective cohorts of patients with (*A*) untreated early-stage NSCLC and (*B*) advanced-stage NSCLC treated with neoadjuvant chemotherapy. Patients were stratified into two groups according to the high/low densities of each marker (*dashed lines* represent the cutoff values). Statistical significance was determined by Spearman test. *Black diamond* = ADC subtype; *gray triangle* = SCC subtype; *white circle* = other subtypes; *white square* = ND. (*C–H*) Kaplan-Meier curves of disease-specific survival for 74 untreated patients with early-stage NSCLC (*C*, *E*, and *G*) and 122 patients with advanced-stage NSCLC treated with neoadjuvant chemotherapy (*D*, *F*, and *H*) according to the densities of $CD20^+$ follicular B cells (Foll-B, *C* and *D*), DC-$Lamp^+$ mature DCs (*E* and *F*), and the combination of both cell populations (*G–H*). The *horizontal dashed lines* represent the median survivals. *P* values were determined using the log-rank test and corrected according to the formula proposed by Altman and coworkers (31). ADC = adenocarcinoma; DSS = disease-specific survival; Foll-B (cell) = follicular B cell; ND = not determined; SCC = squamous cell carcinoma.

Table 2: Prognostic Parameters for Survival in Univariate Analysis for Patients with Untreated Early-Stage Non–Small Cell Lung Cancer

Variable	Class	Hazard Ratio	95% Confidence Interval	*P* Value
Sex	Female	1		
	Male	2.4	0.3–19	0.41
Age	Years	1	0.94–1.1	0.89
Smoking history	<15 pack-years	1		
	>15 pack-years	0.91	0.11–7.3	0.93
Smoking history, pack-years		1	0.97–1	0.99
Histologic subtype	ADC	1		
	SCC	0.61	0.13–3	0.54
pTNM	I	1		
	II	2.2	0.55–8.8	0.26
Tumor differentiation	Well	1		
	Intermediate	0.9	0.15–5.4	0.91
	Poorly	1.2	0.28–5.5	0.78
Fibrosis, %		1	0.97–1	0.93
Necrosis, %		1	0.98–1	0.35
$Ki67^+$ tumor cells, %		1	0.99–1	0.4
Foll-B density	Foll-B high	1		
	Foll-B low	11	1.4–9	**0.02**
DC density	DC high	1		
	DC low	11	2.3–54	**0.003**
Foll-B/DC density	Foll-B/DC high high	1		
	Foll-B/DC mix	8.70×10^8	0 to infinity	NA
	Foll-B/DC low low	2.50×10^9	0 to infinity	NA

Definition of abbreviations: ADC = adenocarcinoma; DC = dendritic cell; Foll-B = follicular B cell; NA = not applicable (because of a lack of events in one group of patients); SCC = squamous cell carcinoma.
The Cox model was used for univariate analysis. A *P* value less than 0.05 was considered statistically significant (bold).

observed in lung tumors. Thus, like in LNs, tumor-infiltrating B cells can organize into fully functional lymphoid structures, as a consequence of B-cell activation.

We evaluated whether the density of follicular B cells correlates with survival of patients with NSCLC, through two retrospective cohorts with distinct characteristics in terms of tumor stage and neoadjuvant treatment. In both cohorts, we demonstrated that a high density of follicular B cells was associated with an increase in the median survival. A positive correlation between B-cell numbers and clinical outcome was previously described in NSCLC (40) and in other cancer types, including primary cutaneous melanoma (41) and breast cancer (42). However, these studies focused on individual tumor-infiltrating B-cell numbers. Here, we analyzed the density of follicular B cells, because it better reflects the initiation of a B-cell response. In that, our strategy parallels the recent work published by Gu-Trantien and coworkers (43), who showed that tumor infiltration by CXCL13-producing $CD4^+$ follicular helper T cells, one of the major partners of follicular B cells in TLS, is associated with organized immune structures and long-term positive clinical outcome in breast cancer. Furthermore, the combination of follicular B-cell and mature DC densities allowed us to identify Foll-B/DC Hi Hi patients with prolonged survival and Foll-B/DC Lo Lo patients at high risk of death. We also observed that combined low densities of mature DCs and $CD8^+$ T cells also defined a group of patients with NSCLC with very poor clinical outcome (44). Likewise, Nielsen and coworkers (45) demonstrated that the presence of both $CD20^+$ and $CD8^+$ tumor-infiltrating lymphocytes correlated with increased survival in high-grade serous ovarian cancer. In light of this study, our results strongly suggest that, in concert with mature DCs, follicular B cells could play a major role in the generation of protective cytolytic immune responses.

In parallel, we evaluated intratumoral B-cell functionality, with a particular focus on their capacity to produce anti-TA Abs. We showed that *ex vivo* cultured B cells were able to produce high levels of IgG and IgA, and that the IgG and IgA produced displayed reactivity against several well-known TAs. Sera reactivities against TAs have been described in many cancer types, such as anti–NY-ESO-1 Abs in sarcoma (46) and primary breast cancer (1), anti–XAGE-1b Abs in NSCLC (3), anti–NY-ESO-1, anti–LAGE1, and anti-P53 Abs in ovarian cancer (37, 45), but the specificity of Abs secreted by tumor-infiltrating B cells has been less investigated. Here, we showed that approximately half of the patients with NSCLC evaluated had developed Ab reactivity against up to seven different TAs, where we identified LAGE-1 as the most immunogenic TA in NSCLC, followed by MAGE family antigens, P53, and NY-ESO-1. In some patients, reactivity against the same TA or additional TAs could be observed in the serum. In addition, the correlations observed in our study between the percentage of PCs and the percentage of GC–B cells in the tumor or the density of follicular B cells in the tumor section strongly suggest that these immunoglobulin-secreting PCs do not come from the periphery but were generated in TLS, after *in situ* antigen-driven B-cell activation. The work of Cipponi and coworkers (47), who identified a series of tumor B-cell clones defined by clonal amplification, SHM, and CSR in metastatic lesions of melanoma, is in accordance with that hypothesis. Finally, a very recent study also pointed out the role

Table 3: Prognostic Parameters for Survival in Univariate Analysis for Patients with Advanced-Stage Non–Small Cell Lung Cancer Treated with Neoadjuvant Chemotherapy

Variable	Class	Hazard Ratio	95% Confidence Interval	*P* Value
Sex	Female	1		
	Male	1.1	0.56–2.2	0.77
Age, years		1	0.97–1	0.96
Smoking history	<15 pack-years	1		
	>15 pack-years	1.6	0.67–3.7	0.3
Smoking history, pack-years		1	1–1	0.21
Histologic subtype	ADC	1		
	SCC	0.5	0.27–0.91	**0.02**
	Others	0.83	0.39–1.8	0.63
	ND	3.7	0.47–29	0.21
pTNM before neoadjuvant chemotherapy	IIIA	1		
	IIIB	1.2	0.52–2.8	0.65
Fibrosis, %		1	0.99–1	0.95
Necrosis, %		0.99	0.98–1	0.2
Viable tumor cells, %		1	1–1	0.2
Side	Left	1		
	Right	1.2	0.67–2.2	0.51
Chemotherapy drugs	CDDP+GC	1		
	CDDP+VIN	1.1	0.6–1.9	0.82
	CDDP+TAX	0.61	0.21–1.8	0.37
	Others	0.9	0.31–2.6	0.85
Time between chemotherapy and surgery, mo		1	0.72–1.4	0.92
pTNM after neoadjuvant chemotherapy	0	NA	NA	NA
	I	1		
	II	4.26	0.9– 20.07	0.067
	IIIA	5.35	1.28–22.28	**0.02**
	IIIB	7.54	1.6–35.6	**0.01**
	IV	NA	NA	NA
Foll-B density	Foll-B high	1		
	Foll-B low	2.1	1.2–3.7	**0.01**
DC density	DC high	1		
	DC low	2.5	1.4–4.5	**0.002**
Foll-B/DC density	Foll-B/DC high high	1		
	Foll-B/DC mix	2.1	0.91–4.7	0.08
	Foll-B/DC low low	4.2	1.9–9.5	**0.0006**

Definition of abbreviations: ADC = adenocarcinoma; CDDP = cisplatin; DC = dendritic cell; Foll-B = follicular B cell; GC = gemcitabine cisplatin; NA = not applicable (because of a lack of events in one group of patients); ND = not determined; SCC = squamous cell carcinoma; TAX = taxotere; VIN = vinorelbine.
The Cox model was used for univariate analysis. A *P* value less than 0.05 was considered statistically significant (bold).

of tumor-infiltrating PCs in NSCLC, by demonstrating the existence of a positive correlation between IgκC expression and longer survival (48).

The existence of such a humoral immune response in some patients with NSCLC opens the way to the development of new vaccine- and antibody-based therapeutic strategies. Several studies reported the development of both humoral and cellular specific immune responses in NY-ESO-1–vaccinated cancer patients (49, 50). In mice, Noguchi and coworkers (51) demonstrated the antitumor effect of an anti–NY-ESO-1 Ab when associated with chemotherapy. They observed not only the generation of an anti–NY-ESO-1 CD8 immune response, but also the differentiation of other antigen-specific $CD8^+$ T cells, thanks to antigen spreading and DC activation by anti–NY-ESO-1 immune complex. Formation of anti-TA immune complex, Fc-γ receptor engagement on DC, and antigen-specific $CD8^+$ T-cell generation (52) could then be one of the main mechanisms underlying TLS B-cell–mediated protective immunity.

In conclusion, we demonstrated that the organization of intratumoral B cells into B-cell follicles is associated with the development of antigen-specific humoral responses, with the emergence of PCs secreting TA-specific immunoglobulins, allowing the identification of new therapeutic targets in NSCLC. In addition, we demonstrated for the first time that the density of follicular B cells is highly predictive of survival in NSCLC, and low densities of both $CD20^+$ and DC-$Lamp^+$ cells allows the identification of patients at very high risk of death. The use of these two strong biomarkers could help clinicians in adjusting treatment strategy for this category of patients. ■

Author disclosures are available with the text of this article at www.atsjournals.org.

Acknowledgment: The authors are grateful to Prs. J. Cadranel, M. Riquet, and P. Bruneval and Drs. M. Antoine and C. Danel from Tenon and European Georges Pompidou hospitals (Paris, France) for their help in the collection of the human samples and clinical data. They thank Ms. M. Gillard-Bocquet, Ms. E. Ritter, Ms. R. Chiu, and Ms. Sarah Nataraj for technical assistance and Ms. E. Devevre, Ms. H. Fohrer-Ting, and Mr. C. Klein from the platform Centre d'Imagerie Cellulaire et de Cytométrie (Cordeliers Research Center, Paris, France) for technical support.

References

1. Hamaï A, Duperrier-Amouriaux K, Pignon P, Raimbaud I, Memeo L, Colarossi C, Canzonieri V, Perin T, Classe J-M, Campone M, *et al*. Antibody responses to NY-ESO-1 in primary breast cancer identify a subtype target for immunotherapy. *PLoS ONE* 2011;6: e21129.
2. Redjimi N, Duperrier-Amouriaux K, Raimbaud I, Luescher I, Dojcinovic D, Classe J-M, Berton-Rigaud D, Frenel J-S, Bourbouloux E, Valmori D, *et al*. NY-ESO-1-specific circulating CD4+ T cells in ovarian cancer patients are prevalently TH1 type cells undetectable in the CD25+FOXP3+Treg compartment. *PLoS ONE* 2011;6:e22845.
3. Ohue Y, Eikawa S, Okazaki N, Mizote Y, Isobe M, Uenaka A, Fukuda M, Old LJ, Oka M, Nakayama E. Spontaneous antibody, and CD4 and CD8 T-cell responses against XAGE-1b (GAGED2a) in non-small cell lung cancer patients. *Int J Cancer* 2012;131:E649–E658.
4. Zippelius A, Gati A, Bartnick T, Walton S, Odermatt B, Jaeger E, Dummer R, Urosevic M, Filonenko V, Osanai K, *et al*. Melanocyte differentiation antigen RAB38/NY-MEL-1 induces frequent antibody responses exclusively in melanoma patients. *Cancer Immunol Immunother* 2007; 56:249–258.
5. Walton SM, Gerlinger M, de la Rosa O, Nuber N, Knights A, Gati A, Laumer M, Strauss L, Exner C, Schäfer N, *et al*. Spontaneous CD8 T cell responses against the melanocyte differentiation antigen RAB38/NY-MEL-1 in melanoma patients. *J Immunol* 2006;177: 8212–8218.
6. Soussi T. p53 Antibodies in the sera of patients with various types of cancer: a review. *Cancer Res* 2000;60:1777–1788.
7. Hanahan D, Weinberg RA. Hallmarks of cancer: the next generation. *Cell* 2011;144:646–674.
8. Fridman WH, Pagès F, Sautès-Fridman C, Galon J. The immune contexture in human tumours: impact on clinical outcome. *Nat Rev Cancer* 2012;12:298–306.
9. Galon J, Costes A, Sanchez-Cabo F, Kirilovsky A, Mlecnik B, Lagorce-Pagès C, Tosolini M, Camus M, Berger A, Wind P, *et al*. Type, density, and location of immune cells within human colorectal tumors predict clinical outcome. *Science* 2006;313:1960–1964.
10. Erdag G, Schaefer JT, Smolkin ME, Deacon DH, Shea SM, Dengel LT, Patterson JW, Slingluff CL Jr. Immunotype and immunohistologic characteristics of tumor-infiltrating immune cells are associated with clinical outcome in metastatic melanoma. *Cancer Res* 2012;72: 1070–1080.
11. Nelson BH. CD20+ B cells: the other tumor-infiltrating lymphocytes. *J Immunol* 2010;185:4977–4982.
12. Rodríguez-Pinto D. B cells as antigen presenting cells. *Cell Immunol* 2005;238:67–75.
13. DeNardo DG, Coussens LM. Inflammation and breast cancer. Balancing immune response: crosstalk between adaptive and innate immune cells during breast cancer progression. *Breast Cancer Res* 2007;9:212.
14. Barbera-Guillem E, Nelson MB, Barr B, Nyhus JK, May KF Jr, Feng L, Sampsel JW. B lymphocyte pathology in human colorectal cancer. Experimental and clinical therapeutic effects of partial B cell depletion. *Cancer Immunol Immunother* 2000;48:541–549.
15. DiLillo DJ, Yanaba K, Tedder TF. B cells are required for optimal CD4+ and CD8+ T cell tumor immunity: therapeutic B cell depletion enhances B16 melanoma growth in mice. *J Immunol* 2010;184: 4006–4016.
16. Tan T-T, Coussens LM. Humoral immunity, inflammation and cancer. *Curr Opin Immunol* 2007;19:209–216.
17. Barbera-Guillem E, May KF Jr, Nyhus JK, Nelson MB. Promotion of tumor invasion by cooperation of granulocytes and macrophages activated by anti-tumor antibodies. *Neoplasia* 1999;1:453–460.
18. Ammirante M, Luo J-L, Grivennikov S, Nedospasov S, Karin M. B-cell-derived lymphotoxin promotes castration-resistant prostate cancer. *Nature* 2010;464:302–305.
19. DeNardo DG, Andreu P, Coussens LM. Interactions between lymphocytes and myeloid cells regulate pro- versus anti-tumor immunity. *Cancer Metastasis Rev* 2010;29:309–316.
20. Simsa P, Teillaud J-L, Stott DI, Tóth J, Kotlan B. Tumor-infiltrating B cell immunoglobulin variable region gene usage in invasive ductal breast carcinoma. *Pathol Oncol Res* 2005;11:92–97.
21. Kotlan B, Simsa P, Teillaud J-L, Fridman WH, Toth J, McKnight M, Glassy MC. Novel ganglioside antigen identified by B cells in human medullary breast carcinomas: the proof of principle concerning the tumor-infiltrating B lymphocytes. *J Immunol* 2005;175:2278–2285.
22. Schmidt M, Böhm D, von Törne C, Steiner E, Puhl A, Pilch H, Lehr H-A, Hengstler JG, Kölbl H, Gehrmann M. The humoral immune system has a key prognostic impact in node-negative breast cancer. *Cancer Res* 2008;68:5405–5413.
23. Dieu-Nosjean M-C, Antoine M, Danel C, Heudes D, Wislez M, Poulot V, Rabbe N, Laurans L, Tartour E, de Chaisemartin L, *et al*. Long-term survival for patients with non-small-cell lung cancer with intratumoral lymphoid structures. *J Clin Oncol* 2008;26:4410–4417.
24. Drayton DL, Liao S, Mounzer RH, Ruddle NH. Lymphoid organ development: from ontogeny to neogenesis. *Nat Immunol* 2006;7: 344–353.
25. Neyt K, Perros F, GeurtsvanKessel CH, Hammad H, Lambrecht BN. Tertiary lymphoid organs in infection and autoimmunity. *Trends Immunol* 2012;33:297–305.
26. Moyron-Quiroz JE, Rangel-Moreno J, Kusser K, Hartson L, Sprague F, Goodrich S, Woodland DL, Lund FE, Randall TD. Role of inducible bronchus associated lymphoid tissue (iBALT) in respiratory immunity. *Nat Med* 2004;10:927–934.
27. Germain C, Tamzalit F, Knockaert S, Gnjatic S, Validire P, Remark R, Damotte D, Fridman WH, Sautes-Fridman C, Dieu-Nosjean MC, *et al*. Intra-tumoral B cells are able to organize into tertiary lymphoid structures and to develop a protective humoral immune response in lung cancer patients. Presented at the 15th International Congress of Immunology, Milan, Italy, August 22–27, 2013.
28. de Chaisemartin L, Goc J, Damotte D, Validire P, Magdeleinat P, Alifano M, Cremer I, Fridman W-H, Sautès-Fridman C, Dieu-Nosjean M-C. Characterization of chemokines and adhesion molecules associated with T cell presence in tertiary lymphoid structures in human lung cancer. *Cancer Res* 2011;71:6391–6399.
29. Gnjatic S, Old LJ, Chen Y-T. Autoantibodies against cancer antigens. *Methods Mol Biol* 2009;520:11–19.
30. Remark R, Alifano M, Cremer I, Lupo A, Dieu-Nosjean M-C, Riquet M, Crozet L, Ouakrim H, Goc J, Cazes A, *et al*. Characteristics and clinical impacts of the immune environments in colorectal and renal cell carcinoma lung metastases: influence of tumor origin. *Clin Cancer Res* 2013;19:4079–4091.
31. Altman DG, Lausen B, Sauerbrei W, Schumacher M. Dangers of using "optimal" cutpoints in the evaluation of prognostic factors. *J Natl Cancer Inst* 1994;86:829–835.
32. van de Pavert SA, Mebius RE. New insights into the development of lymphoid tissues. *Nat Rev Immunol* 2010;10:664–674.
33. Riley JK, Sliwkowski MX. CD20: a gene in search of a function. *Semin Oncol* 2000; 27(6, Suppl 12)17–24.
34. Pascual V, Liu YJ, Magalski A, de Bouteiller O, Banchereau J, Capra JD. Analysis of somatic mutation in five B cell subsets of human tonsil. *J Exp Med* 1994;180:329–339.
35. Caraux A, Klein B, Paiva B, Bret C, Schmitz A, Fuhler GM, Bos NA, Johnsen HE, Orfao A, Perez-Andres M; Myeloma Stem Cell Network. Circulating human B and plasma cells. Age-associated changes in counts and detailed characterization of circulating normal CD138- and CD138+ plasma cells. *Haematologica* 2010; 95:1016–1020.
36. Stockert E, Jäger E, Chen Y-T, Scanlan MJ, Gout I, Karbach J, Arand M, Knuth A, Old LJ. A survey of the humoral immune response of cancer patients to a panel of human tumor antigens. *J Exp Med* 1998;187:1349–1354.
37. Gnjatic S, Ritter E, Büchler MW, Giese NA, Brors B, Frei C, Murray A, Halama N, Zörnig I, Chen Y-T, *et al*. Seromic profiling of ovarian and pancreatic cancer. *Proc Natl Acad Sci USA* 2010;107:5088–5093.
38. Bindea G, Mlecnik B, Tosolini M, Kirilovsky A, Waldner M, Obenauf AC, Angell H, Fredriksen T, Lafontaine L, Berger A, *et al*. Spatiotemporal dynamics of intratumoral immune cells reveal the immune landscape in human cancer. *Immunity* 2013;39:782–795.
39. Gatto D, Brink R. The germinal center reaction. *J Allergy Clin Immunol* 2010;126:898–907, quiz 908–909.
40. Al-Shibli KI, Donnem T, Al-Saad S, Persson M, Bremnes RM, Busund L-T. Prognostic effect of epithelial and stromal lymphocyte infiltration in non-small cell lung cancer. *Clin Cancer Res* 2008;14:5220–5227.

41. Ladányi A, Kiss J, Mohos A, Somlai B, Liszkay G, Gilde K, Fejös Z, Gaudi I, Dobos J, Tímár J. Prognostic impact of B-cell density in cutaneous melanoma. *Cancer Immunol Immunother* 2011;60: 1729–1738.
42. Mahmoud SMA, Lee AHS, Paish EC, Macmillan RD, Ellis IO, Green AR. The prognostic significance of B lymphocytes in invasive carcinoma of the breast. *Breast Cancer Res Treat* 2012;132:545–553.
43. Gu-Trantien C, Loi S, Garaud S, Equeter C, Libin M, de Wind A, Ravoet M, Le Buanec H, Sibille C, Manfouo-Foutsop G, *et al*. CD4+ follicular helper T cell infiltration predicts breast cancer survival. *J Clin Invest* 2013;123:2873–2892.
44. Goc J, Germain C, Vo-Bourgais TKD, Lupo A, Klein C, Knockaert S, de Chaisemartin L, Ouakrim H, Becht E, Alifano M, *et al*. Dendritic cells in tumor-associated tertiary lymphoid structures signal a Th1 cytotoxic immune contexture and license the good positive prognostic value of infiltrating CD8+ T cells. *Cancer Res* 2014;74: 705–715.
45. Nielsen JS, Sahota RA, Milne K, Kost SE, Nesslinger NJ, Watson PH, Nelson BH. CD20+ tumor-infiltrating lymphocytes have an atypical CD27- memory phenotype and together with CD8+ T cells promote favorable prognosis in ovarian cancer. *Clin Cancer Res* 2012;18: 3281–3292.
46. Ayyoub M, Taub RN, Keohan M-L, Hesdorffer M, Metthez G, Memeo L, Mansukhani M, Hibshoosh H, Hesdorffer CS, Valmori D. The frequent expression of cancer/testis antigens provides opportunities for immunotherapeutic targeting of sarcoma. *Cancer Immun* 2004;4:7.
47. Cipponi A, Mercier M, Seremet T, Baurain J-F, Théate I, van den Oord J, Stas M, Boon T, Coulie PG, van Baren N. Neogenesis of lymphoid structures and antibody responses occur in human melanoma metastases. *Cancer Res* 2012;72:3997–4007.
48. Lohr M, Edlund K, Botling J, Hammad S, Hellwig B, Othman A, Berglund A, Lambe M, Holmberg L, Ekman S, *et al*. The prognostic relevance of tumour-infiltrating plasma cells and immunoglobulin kappa C indicates an important role of the humoral immune response in non-small cell lung cancer. *Cancer Lett* 2013;333:222–228.
49. Jäger E, Karbach J, Gnjatic S, Neumann A, Bender A, Valmori D, Ayyoub M, Ritter E, Ritter G, Jäger D, *et al*. Recombinant vaccinia/fowlpox NY-ESO-1 vaccines induce both humoral and cellular NY-ESO-1-specific immune responses in cancer patients. *Proc Natl Acad Sci USA* 2006;103:14453–14458.
50. Bioley G, Guillaume P, Luescher I, Bhardwaj N, Mears G, Old L, Valmori D, Ayyoub M. Vaccination with a recombinant protein encoding the tumor-specific antigen NY-ESO-1 elicits an A2/157-165-specific CTL repertoire structurally distinct and of reduced tumor reactivity than that elicited by spontaneous immune responses to NY-ESO-1-expressing tumors. *J Immunother* 2009;32:161–168.
51. Noguchi T, Kato T, Wang L, Maeda Y, Ikeda H, Sato E, Knuth A, Gnjatic S, Ritter G, Sakaguchi S, *et al*. Intracellular tumor-associated antigens represent effective targets for passive immunotherapy. *Cancer Res* 2012;72:1672–1682.
52. Kalergis AM, Ravetch JV. Inducing tumor immunity through the selective engagement of activating Fcgamma receptors on dendritic cells. *J Exp Med* 2002;195:1653–1659.